Available online at www.sciencedirect.com
SCIENCE DIRECT
Journal of Magnetic Resonance 180 (2006) 256–265
JMR Journal of Magnetic Resonance
www.elsevier.com/locate/jmr

Apparatus for rapid adjustment of the degree of alignment of NMR samples in aqueous media: Verification with residual quadrupolar splittings in ^{23}Na and ^{133}Cs spectra

Philip W. Kuchel [a,*], Bogdan E. Chapman [a], Norbert Müller [b], William A. Bubb [a], David J. Philp [a], Allan M. Torres [a]

[a] School of Molecular and Microbial Biosciences, University of Sydney, NSW 2006, Australia
[b] Institut für Chemie, Johannes Kepler Universität A-4040 Linz, Austria

Received 30 January 2006; revised 3 March 2006
Available online 23 March 2006

Abstract

NMR spectra of $^{23}Na^+$ and $^{133}Cs^+$ in gelatine in a silicone rubber tube that was stretched to various extents showed remarkably reproducible resonance multiplicity. The relative intensities of the components of the split peaks had ratios, 3:4:3, and 7:12:15:16:15:12:7, respectively, that conformed with those predicted using a *Mathematica* program. The silicone-rubber tube was sealed at its lower end by a small rubber stopper and placed inside a thick-walled glass tube. Gelatine was injected in solution into the silicone tube and 'set' by cooling below 30 °C. A plastic thumb-screw held the silicone tube at various degrees of extension, up to ~2-fold. After constituting the gel in buffers containing NaCl and CsCl, both ^{23}Na and ^{133}Cs NMR spectroscopy revealed that after stretching the initial single Lorentzian line was split into a well-resolved triplet and a heptet, respectively. This was interpreted as being due to coupling between the electric quadrupoles of the nuclei and the average electric field gradient tensor of the collagen molecules of gelatine; these molecules became progressively more aligned in the direction of the main magnetic field, $\mathbf{B}_0$, of the vertical bore magnet, as the gel was stretched. This apparatus provides a simple way of demonstrating fundamental physical characteristics of quadrupolar cations, some characteristics of gelatine under stretching, and a way to invoke static distortion of red blood cells. It should be useful with these and other cell types, for studies of metabolic and membrane transport characteristics that may change when the cells are distorted, and possibly for structural studies of macromolecules.

Keywords: Alignment tensor; Electric field tensor; Quadrupolar splitting; Gelatine; Gel; Erythrocytes; 133-Caesium; 23-Sodium

1. Introduction

The tunable alignment of proteins in stretched or compressed gels is a desirable experimental outcome for the determination of protein folds in solution by high resolution NMR spectroscopy [1–4]. The methods employed thus far allow the a priori specification of the extent of alignment, but they do not readily lend themselves to adjustment of this parameter once the sample has been prepared. The standard method [3] involves changing the composition of the gel-solution to adjust the extent of alignment brought about by stretching or compression, and uses a syringe-like device, whose cross-sectional area is larger (or smaller) than that of the tube into which the gel is extruded.

In the present work, we sought a method of inducing anisotropy into NMR samples not only of proteins, but of intact cells. The desirability of the latter is that very little is known about the energetics of maintenance of the shape of cells that undergo extensive in vivo distortion such as the

* Corresponding author. Fax: +61 2 9351 4726.
E-mail address: p.kuchel@mmb.usyd.edu.au (P.W. Kuchel).

1090-7807/$ - see front matter © 2006 Elsevier Inc. All rights reserved.
doi:10.1016/j.jmr.2006.03.002

biconcave human erythrocyte (red blood cell; RBC);[1] or whether membrane transport activity is affected when these cells pass through capillaries [5]. The capillaries have a diameter that is about a half that of the main-diameter of the cell; and since the mean circulation time of an RBC in man is ~1 min, this distortion takes place in the peripheral and pulmonary capillary beds every ~30 s.

In the process of establishing optimal conditions for these experiments, we used a range of gels but settled on gelatine as the medium that was the most convenient to use and compatible with maintaining the cells initially in their normal shape and metabolic state. During this evaluation we needed a means of assessing the stability of the gel to repeated stretching and relaxation and for this we used the quadrupolar splitting of ^{23}Na, seen with natural collagen in cartilage and tendons [6–8], and of another Group I cation, ^{133}Cs. The clarity of the quadrupolar splittings and their reproducibility enabled the degree of extension of the gels to be readily monitored and revealed remarkable stability of the gels to repeated extension and relaxation.

The interpretation of our spectra rested on the theoretical foundations of Brown and Parker [9] and Vega and Pines [10,11]. The elegant early experimental demonstration of residual quadrupolar splitting of the ^{2}H resonance of deuterated benzene in latex elastomers by Deloche and Samulski [12] is a precursor to the present work, although they dealt with an organic-solvent and not the aqueous system we sought. The work is also related to the recent interest in exploiting the special features of quadrupolar cations in clinical diagnosis [13] and in materials science [14,15].

2. Materials and methods

2.1. Chemicals

All fine chemicals were of analytical reagent (AR) grade, and solutions were made using water purified by reverse osmosis. The bovine serum albumin (BSA) was from Sigma (St. Louis, MO) and the gelatine 20 N grade was a gift from Davis Gelatine (Australia) Co. Botany, NSW.

2.2. Stretching apparatus

Fig. 1 shows the device that was used; it consists of a thick-walled glass tube 10.05 mm outside diameter (o.d.), 6.9 mm inside diameter (i.d.), 375 mm long] inside of which was a length of Sims Portex (Hythe, Kent, UK) silicone tubing (7 mm o.d., 5 mm i.d.). A rubber stopper was inserted into the bottom of the silicone tube that in turn was squeezed into the glass tube, and the two were trimmed to leave only a 2 mm length projecting from the bottom. This arrangement was sufficiently firm to ensure that stretching the silicone tube by over a factor of 2 did not detach it.

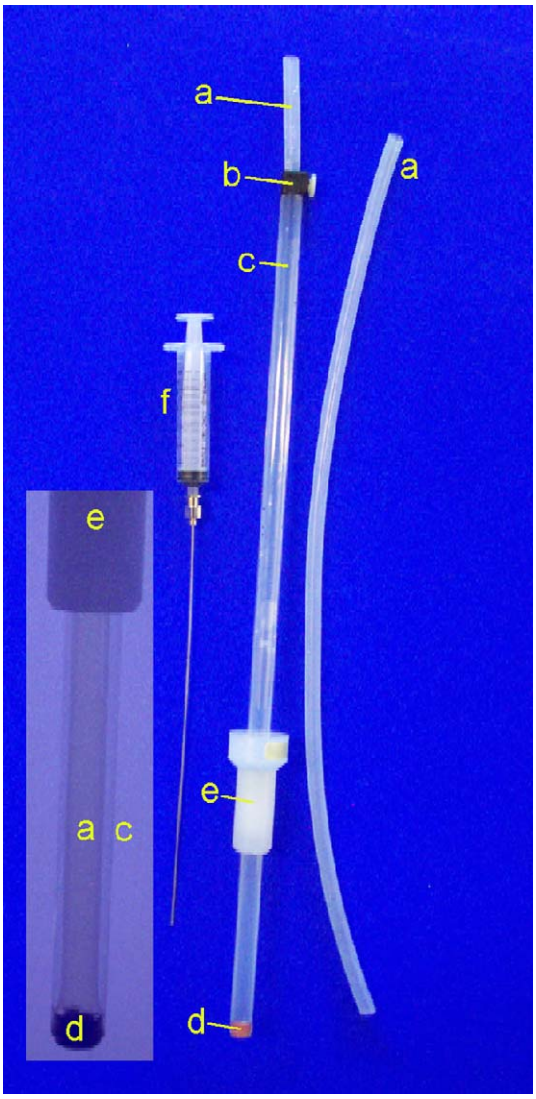

Fig. 1. Device for stretching a gel to any specified length inside a 10-mm glass tube, for NMR studies. The various components are: (a) silicone tube; (b) Delrin (black) clamp with Nylon-screw (white) surrounding the silicone tube; (c) thick-wall glass tube; (d) rubber stopper inside the silicone tube, in turn inside the glass tube, and projecting by ~2 mm; (e) standard NMR-tube spinner used to position the sample inside the NMR probe; (f) 10-mL syringe with a long 21-g needle used to introduce D_2O into the space between (a and c). The inset shows the lower end of the device at higher magnification, showing the distortion that developed at the lower end of the silicone tube when it was stretched; the RF coils were located above this non-uniform region of the sample.

Gelatine (3.5–14% w/v) was constituted in saline and contained BSA (0.055% w/v), and the solution was brought to pH 7.4 with 25–100 μL 5 M NaOH. The BSA was used to ensure that when (in later experiments to be reported elsewhere) RBCs were included in the gel they retained

[1] *Abbreviations used:* BSA, bovine serum albumin; RF, radio frequency; Ht, haematocrit; i.d., inside diameter; o.d., outside diameter; RBC, red blood cell; RF, radiofrequency.

their discocyte shape, as seen by light microscopy; when incorporated, the RBCs were added to the gel at ~44 °C to a final Ht of 16%.

The gelatine/BSA solutions were made up in 20 mL batches and dissolved by heating for 10 s on full-power in a domestic 1 kW microwave oven, achieving a temperature of ~50 °C. More extreme heating conditions led to cloudiness of the gel, due to denaturation of the BSA.

2.3. Experimental set up

The apparatus reported here has the major advantage that the extent of gel stretching is smoothly variable up to a factor of ~2; the latter is determined both by the elastic limit of the tube and the gelatine. The silicone tube that houses the gel was usable for hundreds of stretch-relax cycles and it remained robust after multiple washings in aqueous detergent and ethanol, to promote sterility.

The anchor for the silicone tube within the glass evolved from a rigid Teflon plug to the present small rubber stopper. D_2O was introduced via a syringe (with 24 g × 20 cm needle), to the space between the glass tube and the silicone tube. This diminished magnetic field inhomogeneities by replacing the pocket of air with an aqueous layer that was more similar in magnetic susceptibility to the susceptibilities of silicone and glass [16].

The gelatine was dissolved in buffer in 20 mL batches at ~50 °C and mixed with a spatula and not shaken. Bubbles at the top of the solution were removed by aspiration and the solution allowed to settle for ~1 h at 45 °C before use. The silicone tube was placed within the glass tube and fixed at its lower end by the rubber stopper; and the whole assembly was thermally equilibrated in a water bath at 45 °C. The solution was introduced to the silicone tube via a prewarmed 10 mL disposable syringe with 40 cm of semi-rigid polythene tube, (3.2 mm o.d., and 2.0 mm i.d.). The thumbscrew (**b** in Fig. 1) was tightened on the distal end of the silicone tube and the whole assembly bounced on the laboratory bench several times to dislodge any air bubbles. The thumb-screw was then locked into place at the top of the glass tube and the whole then cooled in ice, or simply placed in a refrigerator at 4 °C for later use. Subsequently, when the gel was stretched to prescribed extents, the length was measured with a ruler having marked the initial position of the silicone tube, level with the top of the glass outer tube, with an indelible pen. The precision of length measurement was ±2 mm.

Because of its weight, the sample was lowered into the vertical bore NMR magnet using cotton tape tied to the upper end of the silicone tube rather than use the usual 'aircushion' facility.

2.4. NMR spectroscopy

The ^{23}Na and ^{133}Cs spectra were recorded at 105.8 and 52.5 MHz, respectively, on a DRX400 NMR spectrometer (Bruker, Karlsruhe, Germany) with an Oxford Instruments (Oxford, UK) 9.4-T vertical wide-bore magnet. A 10-mm broadband probe with thermostatic control was used. The NMR data recording and processing package was XWINNMR (Version 3.5, Bruker). The thermostatic control of the temperature of the sample was calibrated by using a glass capillary containing ethylene glycol and the values reported were accurate to ±1 °C [17].

2.5. Data analysis

Spectra were analyzed using programs written in *Mathematica* (Wolfram Research Inc., Champaign, IL). The experimental spectra in Figs. 2 and 3 were fitted to simulated data with the program PtolemyIII; this program has been developed in-house for spectral simulations and data-fitting used to estimate spectral parameter values [18]. Being written in *Mathematica* the program is similar to that recently reported by Jerschow [19]. The form of the Lorentzian was:

$$\mathrm{lorentz}[\nu 0\_, \mathrm{lw}\_, \nu\_] := \frac{\mathrm{lw}}{2\pi}\frac{1}{(\nu-\nu 0)^2+(\mathrm{lw}/2)^2}, \tag{1}$$

where $\nu 0$ denotes the central frequency (Hz) of the resonance, ν denotes frequency (Hz), and lw is the line width at half the peak height.

The ^{133}Cs spectra were represented by the function, spin7on2quad, as the sum of seven Lorentzians whose relative intensities were given by the leading terms in the following sum.

$$\begin{aligned}&\mathrm{spin7on2quad}[\mathrm{ampl}\_, \nu 0\_, \delta\nu\_, \{\mathrm{lw0}\_, \mathrm{lw1}\_, \mathrm{lw2}\_, \mathrm{lw3}\_\}, \nu\_]:\\ &= \mathrm{ampl}(\mathrm{lorentz}[\nu 0, \mathrm{lw0}, \nu] + \left(\frac{\sqrt{15}}{4}\right)^2(\mathrm{lorentz}[\nu 0-\delta\nu, \mathrm{lw1}, \nu]\\ &+ \mathrm{lorentz}[\nu 0+\delta\nu, \mathrm{lw1}, \nu]) + \left(\frac{\sqrt{3}}{2}\right)^2(\mathrm{lorentz}[\nu 0-2\delta\nu, \mathrm{lw2}, \nu]\\ &+ \mathrm{lorentz}[\nu 0+2\delta\nu, \mathrm{lw2}, \nu]) + \left(\frac{\sqrt{7}}{4}\right)^2(\mathrm{lorentz}[\nu 0-3\delta\nu, \mathrm{lw3}, \nu]\\ &+ \mathrm{lorentz}[\nu 0+3\delta\nu, \mathrm{lw3}, \nu])),\end{aligned} \tag{2}$$

where, ampl denotes the amplitude (arbitrary units) of the central peak in the resonance complex; $\nu 0$ and ν have the same meaning as for Eq. (1); the lw_α values ($\alpha = 0$, 1, 2, 3) are the line-widths at half-peak height of the components of the complex, counting out from the central peak; $\delta\nu$ is the difference in frequency between the central peak and the first adjacent peak in the complex, and so forth, out to the αth component where the splitting is $\alpha \times \delta\nu$; i.e., $\delta\nu$ is the apparent quadrupolar coupling constant; and dd (below) is the List name of the

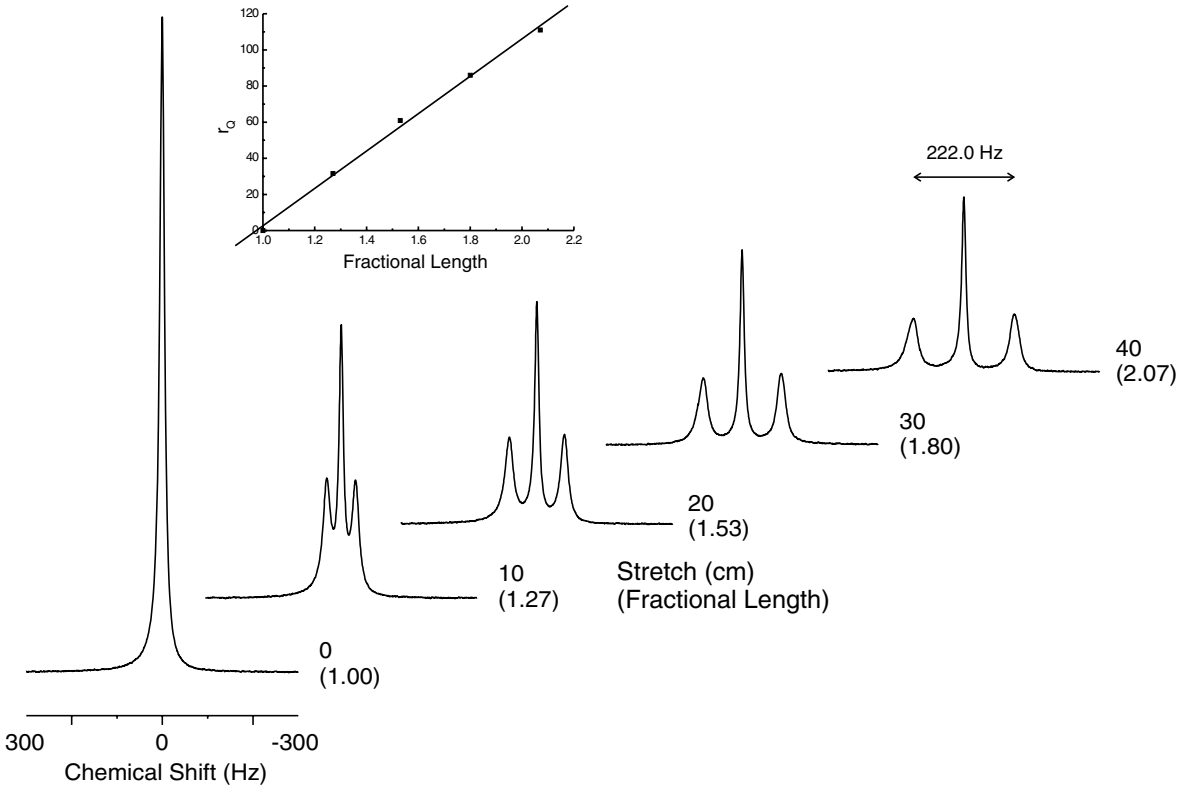

Fig. 2. ^{23}Na NMR (105.8 MHz) spectra of 154 mM NaCl in 14% w/v gelatine, pH 7.4 at 25 °C in the silicone tube, inside the glass tube of 37.5 cm, under various extents of stretching. The spectrum on the far left shows a Lorentzian-shaped resonance assigned the arbitrary chemical shift of 0.00 Hz; the number on the right of each spectrum is the length change in cm, and the number below it, in brackets, indicates the fractional length. The double arrow over the spectrum on the far right indicates the separation in Hz between the two outer components of the triplet; i.e., the value is twice the residual quadrupolar coupling constant, r_Q. The inset shows the magnitude of r_Q (solid squares) as a function of fractional length. The solid line was drawn using linear least-squares regression analysis: $r_Q = (103 \pm 3)$ Hz Fractional Length $- (101 \pm 5)$. NMR acquisition parameters (here and for other figures): 16 transients per spectrum; 8 k data points; pulse-and-acquire RF pulse sequence with ~17 μs $\pi/2$ pulse and standard phase cycling; free-induction decays were apodized using a 3 Hz line-broadening factor.

spectral data set, reduced in size typically to ~130 points. The regression analysis was then done with the following two commands:

$$\ll \text{Statistics}'\text{NonlinearFit}'$$

$$\begin{aligned}&\text{ansNL} = \text{NonlinearRegress}[\text{dd}, \text{spin7on2quad}[\text{ampl}, \nu 0, \delta\nu,\\ &\{\text{lw0}, \text{lw1}, \text{lw2}, \text{lw3}\}, \nu\}, \nu, \{\{\text{ampl}, 10^9\}, \{\nu 0, 280\}, \{\delta\nu, 3\},\\ &\{\text{lw0}, 1.5\}, \{\text{lw1}, 1.5\}, \{\text{lw2}, 1.5\}, \{\text{lw3}, 1.5\}\}]\end{aligned} \tag{3}$$

where the first line calls the Standard Add-On Package for nonlinear regression analysis and second line executes the algorithm.

The output of the function, ansNL, was a table showing the estimates of each of the six parameter-values, and their standard deviations (see captions of Figs. 4 and 5 for values).

The ^{23}Na spectra were represented as the sum of three Lorentzian components of relative intensity given by the leading term in the above sum, and with only the lw0 and lw1 symbols in the argument list. Where relevant in some regressions (e.g., Fig. 5), a baseline offset parameter was included in the argument list.

2.6. Theory of resonance multiplicity and methods of calculation–physical rationale

An understanding of the relative intensities of the components of the resonances of ^{23}Na and ^{133}Cs is needed for an appreciation of how close to "ideal" the spectra were. Only a quantum mechanical description successfully accounts for the resonance/peak multiplicity and the relative intensities evident in the NMR spectra of quadrupolar nuclei in the kind of system used in the present work [9–12,20]. Because of its specialized nature the details of the formally correct way [20–22] of calculating the ideal spectra that were used in the fitting analysis are placed in Appendix A. On the other hand a heuristic, or physical, intuition relating to such systems is worth achieving, and it is as follows.

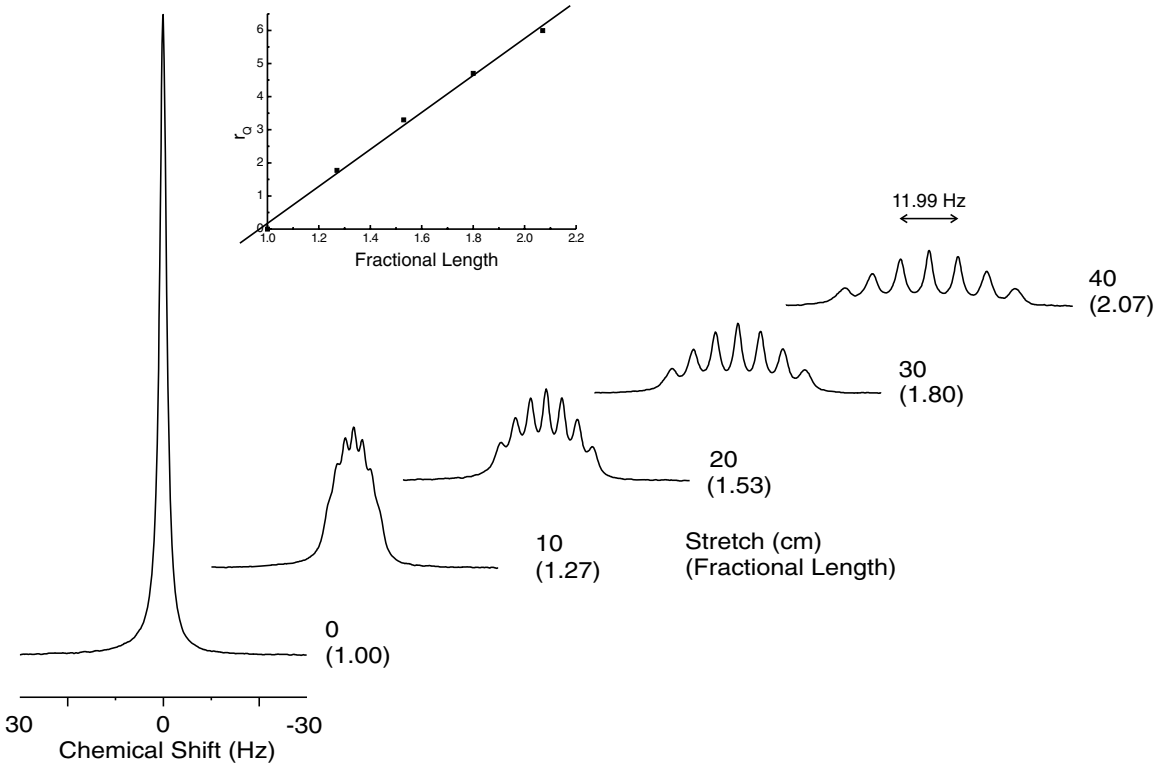

Fig. 3. ^{133}Cs NMR spectra of 154 mM CsCl in 14% w/v gelatine, pH 7.4 at 25 °C in the silicone tube, inside the glass tube of 37.5 cm, under various extents of stretching. The spectrum on the far left shows a Lorentzian-shaped resonance given an arbitrary chemical shift of 0.00 Hz; the number on the right of each spectrum is the length change in cm, and the number below it, in brackets, indicates the fractional length. The spectrum on the far right has a double arrow associated with it, indicating the separation in Hz between the two inner components on either side of the central peak of the heptet; i.e., the value is twice the residual quadrupolar-coupling constant, r_Q. The inset shows the magnitude of r_Q (solid squares) as a function of fractional length. The solid line was drawn using linear least-squares regression analysis: $r_Q = (5.6 \pm 0.2\ \text{Hz})$ Fractional Length $- (5.4 \pm 0.3)$.

For an ensemble of isolated spin $= I$ nuclei (hereafter called spins) in a uniform magnetic field there are $2I + 1$ eigenstates or energy levels available to the spins. For an isotropic sample the energy difference between any two adjacent states is the *same*, so the energy gain or loss of a spin when promoted from one state to another adjacent state is the same between all states. Because of the low energy of these 'Zeeman' states, relative to thermal energy, they are populated (according to Boltzmann) in such a way that the difference in numbers of spins from one state to the next is effectively the same for all the states.

There are $2I$ single-quantum energy differences in the ensemble, and according to Planck's Law the resonance frequency of a transition is the same for each transition; this degeneracy (of transition energies between states) yields an NMR spectrum that is a single peak, even though transitions between all energy levels take place when RF quanta at the appropriate (Larmor) resonance frequency are applied to the system. However, the numbers of spins that move between adjacent energy levels differs from one level to the next. To understand this, consider an $I = 7/2$ system, relevant to ^{133}Cs.

There are 8 energy levels populated by spins in the proportions, 10:20:30:40:50:60:70:80 giving a total number of spins that is proportional to this sum, 360. Thus the difference in number of spins between each adjacent pair of states is proportional to 10. An RF pulse at the resonance frequency, applied for sufficient duration to bring about a 90° nutation of the bulk magnetization vector, equalises the numbers of spins in each energy level to 45. (Aside: this is not tantamount to magnetic saturation, as the propagated spins are rendered coherent in their phases by the RF field, so they are quantum mechanically distinguishable.) Hence, for the lowest energy level with 80 spins, ***35*** (net) are propagated up, leaving behind 45, and this next level up then contains $70 + 35 = 105$ spins. This level loses ***60*** spins to the next level up, leaving behind 45, and the next level up then contains $60 + 60 = 120$ spins; this loses ***75*** spins to the next level up that then has $75 + 50 = 125$; this loses ***80*** spins and these 80 spins add to the 40 in the next level up to give 120 from which ***75*** propagate to the next level up; which then has $75 + 30 = 105$ spins; from this level ***60*** spins move up to the next level that has $60 + 20 = 80$ spins and from this ***35*** move up to the highest energy level giving a total of 45 spins there.

The ratios of the numbers of spins transferred between adjacent levels (bold italics numbers, above) is ***35:60:75:80:75:60:35*** which is divisible by 5 to give relative intensities of the 7 transitions of 7:12:15:16:15:12:7.

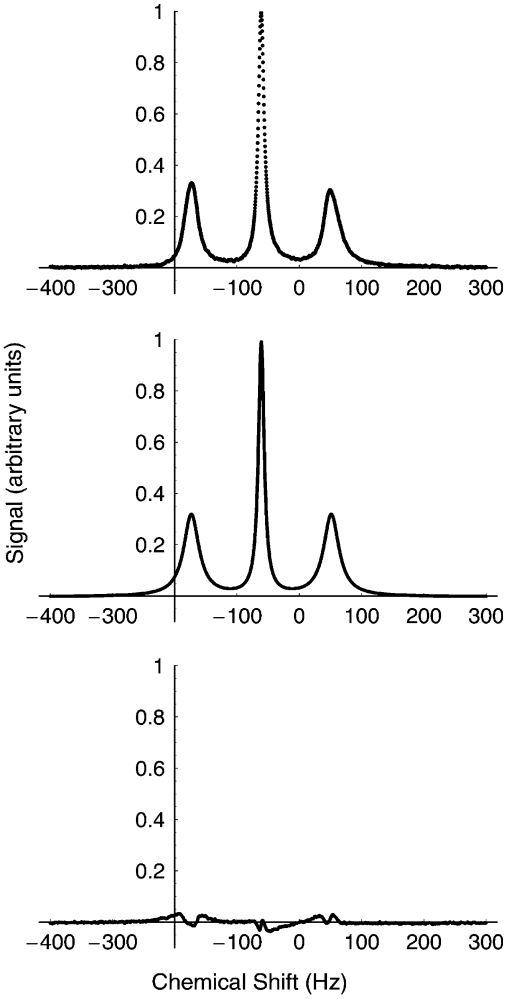

Fig. 4. Nonlinear least squares regression analysis of ^{23}Na NMR spectra (105.8 MHz) of 75 mM NaCl and 75 mM CsCl, in 14% w/v gelatine, stretched in the apparatus shown in Fig. 1 at 25 °C. The top panel shows the raw data from the right-hand spectrum of Fig. 2 for which the gelatine was stretched by a factor of 2.07. The central panel shows the *Mathematica*-based fit to the data of the three-Lorentzian counterpart of Eq. (3) (the general form is given in Eq. (A3)) modified to include a baseline off-set. NonlinearRegress gave estimates of the standard deviations. The lower panel is a plot of the residuals between the raw data and the fit. The values of the parameters and their standard deviations were: ampl $= (4.86 \pm 0.01) \times 10^9$; baseline off-set $= -(1.67 \pm 0.01) \times 10^{-4}$; $\nu 0 = -60.95 \pm 0.02$; $\delta\nu = 112.34 \pm 0.06$ Hz; lw0 $= 11.07 \pm 0.04$ Hz; lw1 $= 29.6 \pm 0.1$ Hz.

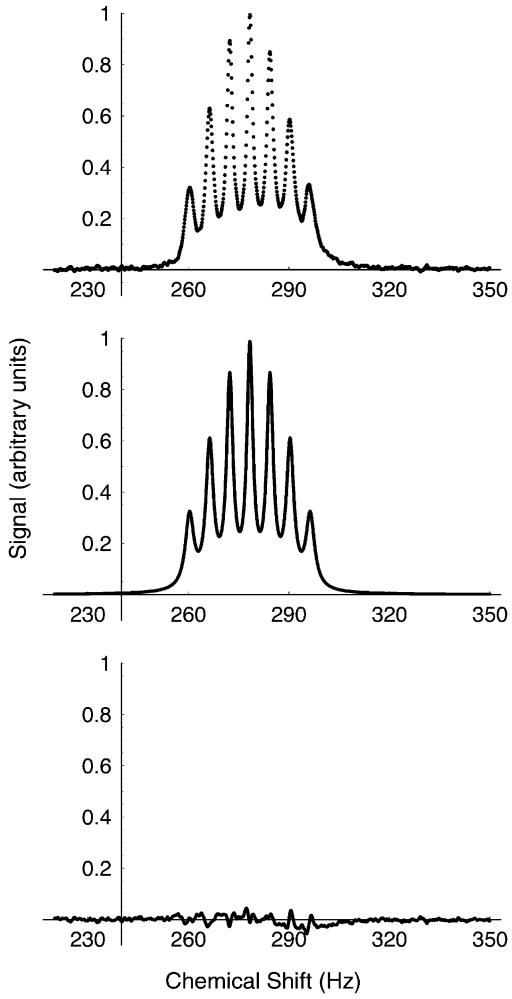

Fig. 5. Nonlinear least squares regression analysis of ^{133}Cs NMR spectra (52.5 MHz) of the sample used for Fig. 4. The top panel shows the raw data from the right-hand spectrum of Fig. 3 for which the gelatine was stretched by a factor of 2.07. The central panel shows the *Mathematica*-based fit to the data of the seven-Lorentzian expression given in Eq. (2) (the general form is given in Eq. (A2)). NonlinearRegress gave estimates of the standard deviations. The lower panel is a plot of the residuals between the raw data and the fit. The values of the parameters and their standard deviations were: ampl $= (1.647 \pm 0.003) \times 10^9$; $\nu 0 = 278.375 \pm 0.003$; $\delta\nu = 5.999 \pm 0.003$ Hz; lw0 $= 2.17 \pm 0.02$ Hz; lw1 $= 2.34 \pm 0.1$ Hz; lw2 $= 2.70 \pm 0.01$ Hz; lw3 $= 3.06 \pm 0.03$ Hz.

The argument thus far has considered equal energy differences between the eigenstates. However differences are introduced by the interaction of the nuclear electric quadrupole with an electric field gradient in the sample. In the situation where the principal axis of the time-averaged electric field gradient tensor in the sample is non-zero, and the spins are freely mobile, the differences in energy between the 8 eigenstates are all different. In special cases like that encountered in the experiments described in the present paper the energy perturbation brought about by the quadrupolar interaction (10 s of Hz only) is very much smaller relative to the Zeeman energy (Larmor frequency, millions of Hz) so the Boltzmann distribution of spins in the 8 populations is not significantly perturbed. Therefore the NMR resonance will be split, to a high level of precision, according to the above ratios; and any deviation in experimental spectra from this ratio can be ascribed to inhomogeneity in the sample (see Section 4).

3. Results

3.1. Stretching apparatus

The experimental apparatus shown in Fig. 1 has several features that distinguish it from other devices that stretch

gels for NMR experiments [1–4]. The most frequently used one is a screw-driven syringe with a barrel whose cross-sectional area is a given factor larger than that of the outlet via a truncated cone at the end of the syringe [3]. The extruded gel passes in an uninterrupted way into a glass tube that is held firmly in the outlet. The extent of stretching (called the 'extension ratio' by Deloche and Samulski [12]) is proportional to the ratio of the cross-section of the syringe barrel and the sample tube. In the present device the extent of stretching was smoothly variable up to a factor of ~2. Provided the concentration of the gelatine was sufficiently high, the gel did not fragment and the silicone tube and gel relaxed to their original length with no physical distortion to either component.

3.2. $^{23}Na^+$ quadrupolar splitting

Fig. 2 shows a typical series of ^{23}Na NMR spectra obtained from 75 mM NaCl in gelatine with various extents of stretching. Note the uniform and symmetrical emergence of a triplet structure from the previous Lorentzian singlet when the gel was stretched. All these spectral patterns were highly reproducible; the quadrupolar splitting at a given length was obtained again after the gel was relaxed back to that length. The inset of Fig. 2 shows a linear relationship (within experimental error) between the residual quadrupolar splitting and the extension ratio of the gel.

Peak splitting was also a function of the gelatine concentration: e.g., at 25 °C for gelatine at 3.5, 7, and 17% w/v the value of the splitting at a length change of 2.07 was 23, 53, and 112 Hz, respectively. The extent of peak splitting at any given length of stretching was independent of the NaCl concentration.

3.3. $^{133}Cs^+$ quadrupolar splitting

Fig. 3 shows a series of ^{133}Cs NMR spectra obtained from 75 mM CsCl in gelatine (same sample as in Section 3.2; with 75 mM NaCl also present) with various extents of stretching. As for $^{23}Na^+$ there was a linear relationship (within experimental error) between the splitting and the extent of stretching of the gel. The value of a splitting was highly reproducible and obtained again after stretching and relaxing back to a given length of the gel.

3.4. Quantification

While the spectra from both nuclides were very well-defined it was not immediately obvious that the components of each resonance were of the theoretically 'ideal' relative intensities. It is well-established that the relative intensities of the three peaks in a resolved $^{23}Na^+$ signal have the ratios 3:4:3 [23]. This was confirmed de novo by using PtolemyIII, which was also used to predict the situation for $^{133}Cs^+$ (see Section 2.5 and Appendix A). For the latter, the intensity ratios were predicted to be 7:12:15:16:15:12:7. The experimental spectra shown in Figs. 2 and 3 therefore were assessed for closeness of fit to the formulae for the ideal spectra; the fits are given in Fig. 4 for $^{23}Na^+$ and Fig. 5 for $^{133}Cs^+$. It is clear from the plots of the residuals between the experimental and fitted data that the experimental data were very close to 'ideal'. In other words, the experimental system produced a homogenous sample in which a single function, with realistic coupling constants, applied. It is evident from inspection of Fig. 4 that the outer peaks are almost identical in size and shape and over twice as wide at half their height, as the central one; nonlinear regression analysis yielded values for the line-widths of the central and two outer components of 11.07 ± 0.04 and 29.6 ± 0.1 Hz, respectively.

As shown in Fig. 5, a single function also described the $^{133}Cs^+$ spectrum. The linewidths of the central component and three components on each side of it were 2.17 ± 0.02, 2.34 ± 0.1, 2.70 ± 0.01, and 3.06 ± 0.03 Hz, respectively. Thus, the linewidths of the components of the multiplets monotonically increased up to 41% for the lowest and highest frequency components. This was a much less dramatic effect than the 167% difference seen in the $^{23}Na^+$ spectrum from the same sample.

4. Discussion

4.1. Stretching apparatus

The major advantage of our device, over others that stretch gels for NMR work, is the ability to rapidly adjust the degree of alignment experienced by the reporter nuclei. Gelatine may be difficult to use for providing an asymmetric environment for protein structure determination, as the spectral signature of collagen is likely to obscure some of those from proteins of interest. On the other hand, the basic arrangement of a silicone tube inside a glass tube to house the gel and thus provide stable elongation of the gel is likely to be useful with other gel types such as acrylamide [1–4]. However, this arrangement would not easily allow the soaking of the gel in a protein solution to load it after the gel had been cast; this was not a concern when dealing with cells that needed to be cast in the gel from the outset.

Other considerations are the compromised filling factor due to the two layers of tubing around the sample, and signals from silicone rubber that are fairly intense and may interfere with shimming. However, these aspects were not problematic in the present studies.

The gel-sample used for both Figs. 2 and 3 was the same, so errors in the estimation of the fractional length change are expected to be the same for both data sets. This accounts for the slight systematic curvature of the data relative to the fitted line in each case (see the insets of Figs. 2 and 3). Whether there is a cause of the curvature other than experimental error awaits further experience with the system. However, it was possible routinely to reselect a given

extent of stretching and record a splitting that was within 1 Hz of the previously recorded value.

4.2. Motivation

The motivation for the experiments was the establishment of a systematic means of periodically distorting the shapes of RBCs to study possible changes in metabolic and membrane transport function. The present results convincingly demonstrated that the gelatine developed significant, reproducible, alignment in the direction of the main magnetic field of the NMR spectrometer when stretched. The proof that RBCs that were incorporated into the gelatine also became distorted by stretching will be reported elsewhere, as will the effects of this distortion on both metabolic and membrane transport processes.

4.3. Other gels

Gelatine was the preferred elastomer because of its compatibility with cells. Notwithstanding this feature, the gelatine needed careful adjustment of pH to bring it up to the physiological range. Attempts to use agarose, another biocompatible gel, failed because it is much less extensible than gelatine. When solidified, low-melting temperature-agarose was stretched by ~10% the column of gel became fragmented into short sections, on the millimeter scale, with intervening sections of free buffer. No evidence of residual quadrupolar splitting of either the $^{23}Na^{+}$ or the $^{133}Cs^{+}$ signals was seen (results not shown). Attempts to use the Ca^{2+}-polymerized gel, alginate, were even less successful, largely because of the difficulty of uniformly mixing alginate and the cation when casting the gel in the silicone tube. Furthermore, such carbohydrate gels were seen to have low extensibility (results not shown).

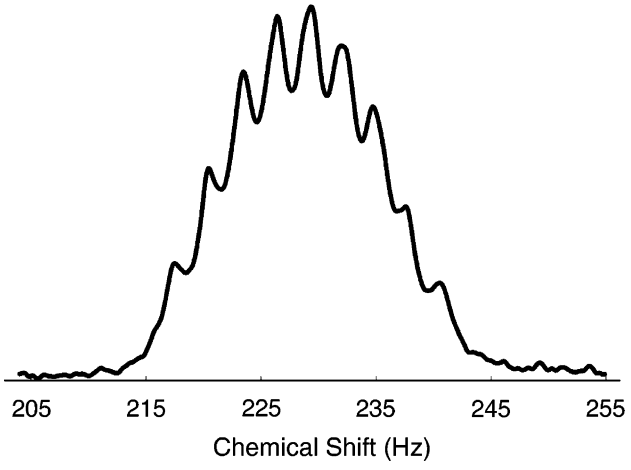

Fig. 6. Un-resolved nine-component (nonet) NMR (52.5 MHz) multiplet from 75 mM $^{133}Cs^{+}$ in 7% w/v gelatine, stretched by a factor of 2, at 25 °C. The nonet (as opposed to the septets in Figs. 3 and 5) is an artefact of fragmentation of the gel. The fragmentation was easily seen by unaided visual inspection.

4.4. Artefacts

The tensile strength of a gelatine gel varies with its concentration, temperature and other factors such as pH and buffer composition [24]. In most cases structural failure of the gel was manifest in the spectra as a marked broadening and loss of resolution of the multiplets. However, on some occasions a series of changes occurred that led to artefacts such as that shown in Fig. 6, in which a high level of coherence was maintained in the multiplet structure of the spectrum, giving a nonet; theoretically, such a spectrum would arise with a nuclide of spin $I = 9/2$! However on close inspection the sample was seen to have separated into gel and free aqueous regions; and yet to give rise to superimposed and shifted septets there must have been predominantly two regions of gel with a high level of retained order, while the free-aqueous regions would have added signal to the central singlet.

This example underscores the need to be alert to tell-tale signs that a gel has fragmented. Nevertheless, the most common outcome of such gel failure was simply peak broadening and a loss of definition of the usual multiplet structure in the spectrum.

4.5. Conclusions

The very close conformity of the splitting patterns of the $^{23}Na^{+}$ and $^{133}Cs^{+}$ spectra to theoretical predictions (Eqs. (A2) and (A3)), and their reproducibility, attested to the remarkable stability of the gelatine gel and its cross-linking. The gelation process is mediated by hydrogen bonds whose formation is favored at lower temperatures, and the gel is expected to be stable below 30 °C. There is an extensive literature on the mechanical properties of gelatine gels [24]. The present analysis adds another, more fundamental, approach to this characterization. Since most nuclei of the Periodic Table are quadrupolar [23] it is likely that splitting patterns, based on the values of their spin quantum numbers, will emerge in stretched gels, like those shown here. A particularly accessible case is likely to be ^{2}H whose splitting patterns have already been shown to vary with degree of extension of polyisoprene constituted in deuterated organic solvents [12].

Acknowledgments

The work was funded by a Discovery Grant from the Australian Research Council to P.W.K. and by the Austrian Science Funds (Project P15380) to N.M. We are grateful to Dr. Wolfgang Bermel (Bruker BioSpin) for valuable discussions and assistance with probe technology. Ces Dela Paz and Ross Taylor are thanked for expert workshop assistance, and Bill Lowe is thanked for expert laboratory input. P.W.K. thanks the Australian Academy of Science for a Europe Exchange Fellowship to the Department of Chemistry, Johannes Kepler University, Linz; and staff and students there are acknowledged for valuable assistance.

Appendix A. Symbolic computation describing quadrupolar split spectra

The relative intensities of the components of the septet that are formed in the case of residual quadrupolar splitting of ^{133}Cs were derived by using density matrix theory (e.g., [20]). We used the fact that the expectation value of the x, y-plane magnetization, I_-, of such a system of isolated Spin = 7/2 nuclei, after a period of evolution under the quadrupolar Hamiltonian, is given by the trace of the matrix product of the density matrix and I_-. The sequence of commands used in *Mathematica* with PtolemyIII was:

$$\begin{aligned}
&1.\ \ll \mathrm{PtolemyIII}'\\
&2.\ \mathrm{SetOptions}[\mathrm{SpinSystems}, \mathrm{SpinList} \rightarrow \{7/2\},\\
&\quad \mathrm{SpinLabels} \rightarrow \text{“Cs”}]\\
&3.\ \mathrm{HQ}_1[1, \mathrm{SpinList} \rightarrow \{7/2\}]\\
&4.\ \mathrm{HQ}_1//\mathrm{OperatorToMatrix}//\mathrm{MatrixForm}\\
&5.\ \mathrm{AddAllEvolveRules}[\lambda_-, \mathrm{T}_{2,0}^{7/2}];\\
&6.\ \sigma 0 = \mathrm{T}_{1,0,0}^{7/2};\\
&7.\ \sigma 0 \overset{\mathrm{Ix}_1\pi/2}{\rightarrow} \sigma 1;\\
&8.\ \sigma 1 \overset{\mathrm{q\ t}H\mathrm{Q}_1}{\rightarrow} \sigma 2;\\
&9.\ \mathrm{im} = \mathrm{IMinus}_1//\mathrm{OperatorToMatrix}\\
&10.\ \mathrm{expectation} = \mathrm{Tr}[\sigma 2.\mathrm{im}]//\mathrm{Simplify},
\end{aligned} \tag{A1}$$

where the sequence of commands from the first to the tenth line entailed: (1) a call to load PtolemyIII into the *Mathematica* kernel; (2) specification on the nuclear system, Cs, and its spin quantum number, 7/2; (3) call on the quadrupolar Hamiltonian that is already defined in general in PtolemyIII; (4) printout of the matrix form of the Hamiltonian (optional); (5) execution of a procedure to list in the *Mathematica* kernel all rules that describe the evolution of the density matrix; (6) specification of the initial state of nuclear polarization, represented as a modified spherical tenor (e.g., [21]); (7) operation on this initial density matrix with a $\pi/2$ pulse around the x-axis in the rotating NMR frame of reference; (8) evolution of the density matrix under the quadrupolar Hamiltonian with q being a scalar of unspecified value but intended to represent the main term in the expression in e.g., [14]; note, the arrow notation used to invoke time-dependent evolutions is interpreted by PtolemyIII, that then applies the relevant tensor transformation rules; (9) define the I_ operator whose expectation value defines the acquired NMR signal; and (10) the expectation is calculated here and output is in symbolic (not numerical) form.

The output was:

$$\frac{1}{2\sqrt{42}}(ie^{-6i\pi qtvQ_1}(7 + 12e^{2i\pi qtvQ_1} + 15e^{4i\pi qtvQ_1} + 16e^{6i\pi qtvQ_1} + 15e^{8i\pi qtvQ_1} + 12e^{10i\pi qtvQ_1} + 7e^{12i\pi qtvQ_1})). \tag{A2}$$

This expression indicates that the magnetization is a sum of exponentials raised to complex powers (hence they denote periodic functions, according to Euler's theorem) with periods of 1, 2, 3, 4, 5 and 6/(q t vQ_1). The Fourier transform of this function, as a function of time, gives seven peaks with relative intensities 7:12:15:16:15:12:7.

Similarly, for the analysis of ^{23}Na (Spin = 3/2), the output showed the familiar [23] peak intensity ratio of 3:4:3,

$$\frac{1}{2\sqrt{5}}(ie^{-2i\pi qtvQ_1}(3 + 4e^{2i\pi qtvQ_1} + 3e^{4i\pi qtvQ_1})). \tag{A3}$$

This output is a very general expression that provides the answer to the question "What are the relative amplitudes of the components in the multiplet?" The relative amplitudes were then explicitly declared in the formulae used for regression analysis, described in Section 2.5.

References

[1] R. Tycko, F.J. Blanco, Y. Ishii, Alignment of biopolymers in strained gels: a new way to create detectable dipole–dipole couplings in high-resolution biomolecular NMR, J. Am. Chem. Soc. 122 (2000) 9340–9341.

[2] H.-J. Sass, G. Musco, S.J. Stahl, P.T. Wingfield, S. Grzesiek, Solution NMR of proteins within polyacrylamide gels: diffusional properties and residual alignment by mechanical stress or embedding of oriented purple membranes, J. Biomol. NMR 18 (2000) 303–309.

[3] J.J. Chou, S. Gaemers, B. Howder, J.M. Louis, A. Bax, A simple apparatus for generating stretched polyacrylamide gels, yielding uniform alignment of proteins and detergent micelles, J. Biomol. NMR 21 (2001) 377–382.

[4] J.J. Chou, J.D. Kaufman, S.J. Stahl, P.T. Wingfield, A. Bax, Micelle-induced curvature in a water-insoluble HIV-1 Env peptide revealed by NMR dipolar coupling measurement in stretched polyacrylamide gel, J. Am. Chem. Soc. 124 (2002) 2450–2451.

[5] P.W. Kuchel, Gh. Benga, Why does the mammalian red blood cell have aquaporins? BioSystems 82 (2005) 192–196.

[6] U. Eliav, G. Navon, Analysis of double-quantum-filtered NMR spectra of ^{23}Na in biological tissues, J. Magn. Reson. B. 103 (1994) 19–29.

[7] G. Navon, H. Shinar, U. Eliav, Y. Seo, Multiquantum filters and order in tissues, NMR Biomed. 14 (2001) 112–132.

[8] U. Eliav, K. Keinan-Adamsky, G. Navon, A new method for suppressing the central transition in $I = 3/2$ NMR spectra with a demonstration for ^{23}Na in bovine articular cartilage, J. Magn. Reson. 165 (2003) 276–281.

[9] L.C. Brown, P.M. Parker, Nuclear magnetic dipole and electric quadrupole energy relations, Phys. Rev. 100 (1955) 1764–1767.

[10] S. Vega, A. Pines, Operator formalism for double quantum NMR, J. Chem. Phys. 66 (1977) 5624–5644.

[11] S. Vega, Fictitious spin 1/2 operator formalism for multiple quantum NMR, J. Chem. Phys. 68 (1977) 5518–5527.

[12] B. Deloche, E.T. Samulski, Short-range nematic-like orientational order in strained elastomers: a deuterium magnetic resonance study, Macromolecules 14 (1981) 575–581.

[13] U. Duvvuri, J.S. Leigh, R. Reddy, Detection of residual quadrupolar interaction in human breast in vivo using sodium-23 multiple quantum spectroscopy, J. Magn. Reson. Imag. 9 (1999) 391–394.

[14] M. Edén, Computer simulations in solid-state NMR.I. Spin dynamics theory, Concepts Magn. Reson. A. 17A (2005) 117–154.

[15] R. Kumar, W. Ling, W. Schoefberger, A. Jerschow, Separated quadrupolar field experiment, J. Magn. Reson. 172 (2005) 209–213.

[16] P.W. Kuchel, B.E. Chapman, W.A. Bubb, P.E. Hansen, C.J. Durrant, M.P. Hertzberg, Magnetic susceptibility: solutions, emulsions, and cells, Concepts Magn. Reson. 18A (2003) 56–71.

[17] W.A. Bubb, K. Kirk, P.W. Kuchel, Ethylene glycol as a thermometer for X-nucleus spectroscopy in biological samples, J. Magn. Reson. 77 (1988) 363–368.

[18] D.J. Philp, P.W. Kuchel, A way of visualizing NMR experiments on quadrupolar nuclei, Concepts Magn. Reson. 25A (2005) 40–52.
[19] A. Jerschow, MathNMR: spin and spatial tensor manipulations in Mathematica, J. Magn. Reson. 176 (2005) 7–14.
[20] P.J. Hore, J.A. Jones, S. Wimperis, NMR: The Toolkit, Oxford University Press, Oxford, 2000.
[21] R. Kemp-Harper, D.J. Philp, P.W. Kuchel, Nuclear magnetic resonance of *J*-coupled quadrupolar nuclei: use of the tensor operator product basis, J. Chem. Phys. 115 (2001) 2908–2916.
[22] A. Abragam, The Principles of Nuclear Magnetism, Clarendon Press, Oxford, 1961, p. 249 Eq. (45).
[23] W.D. Rooney, C.S. Springer, A Comprehensive approach to the analysis and interpretation of the resonances of spins 3/2 from living systems, NMR Biomed. 4 (1991) 209–226.
[24] A.G. Ward, A. Courts (Eds.), The Science and Technology of Gelatin, Academic Press, London, 1977.